QoS Constrained Pilot Allocation Scheme for Massive MIMO Systems

Chenhao Qi, *Senior Member, IEEE*,
Xuyao Sun, *Student Member, IEEE*,
Yansha Deng, *Member, IEEE*,
and Arumugam Nallanathan, *Fellow, IEEE*

***Abstract*—Different from the existing works, in this paper we investigate the pilot allocation in multi-cell massive multiple-input multiple-output (MIMO) systems, aiming to maximize the spectral efficiency (SE) subject to the constraint that the number of user equipments (UEs) satisfying the quality of service (QoS) is maximized. Since the considered bilevel optimization problem that is tough to handle, we resort to the greedy algorithms with low computational complexity. We propose a QoS constrained (QC) pilot allocation scheme, which sequentially allocates the pilot sequence having large interference power to the UE with small signal power so that the number of UEs satisfying QoS can be maximized and then the SE can also be maximized. Simulation results show that the propose QC scheme outperforms the conventional scheme and smart pilot allocation (SPA) scheme.**

***Index Terms*—Channel estimation, massive MIMO, pilot allocation, quality of service (QoS).**

I. Introduction

The next generation wireless communications involve many candidate technologies, including millimeter wave (mmWave) communications [1], [2], machine-learning-based intelligent communications [3], [4], non-orthogonal multiple access (NOMA) [5], [6], massive multiple-input multiple-output (MIMO) [7], [8], and etc. Among them, massive MIMO that attracts great research interests has already been commercially deployed. Massive MIMO typically using many antennas at the base station (BS), can bring significant performance improvement in spectral efficiency (SE) and energy efficiency (EE). As the number of BS antennas grows without limit, asymptotic analysis demonstrates that the effects of uncorrelated noise and fast fading vanish. However, the inter-cell interference due to the reuse of the pilot sequences in other cells, known as pilot contamination [9], still remains even if the number of BS antennas goes to infinity. Pilot contamination has been regarded as one critical performance bottleneck in massive MIMO systems limiting the further increase of the system capacity [10].

To reduce the pilot contamination in massive MIMO, some recent works on pilot allocation has been presented. By exploring the large-scale property of wireless channels, a smart pilot allocation (SPA) scheme is proposed to improve the worst uplink signal-to-interference-plus-noise ratio (SINR) among all user equipments (UEs) in the target cell [11]. Specifically, the SPA scheme sequentially allocates the pilot sequence with the smallest inter-cell interference to the UE having the worst channel quality. In [12], the pilot allocation problem is formulated as a minimum-weight multi-index assignment problem, which is then solved by the Hungarian algorithm with a tractable computational complexity. In [13], a deep learning-based pilot allocation scheme (DL-PAS) is proposed to reduce the pilot contamination. By learning the relation between pilot allocation and location pattern of the UEs, DL-PAS can improve the SE performance of cellular networks that have severe pilot contamination. In [14], a weighted-graph-coloring-based pilot decontamination scheme is proposed to mitigate the pilot contamination for multicell massive MIMO systems, where an edge-weighted interference graph is constructed to depict the potential pilot contamination among users. However, none of these works consider the quality of service (QoS), which is an important metric in practice to guarantee the basic requirement of UEs.

In this work, different from the existing works, we aim to maximize the SE subject to the constraint that the number of the UEs satisfying the QoS is maximized, by designing the pilot allocation scheme to alleviate the pilot contamination in multi-cell massive MIMO systems. For the considered bilevel optimization problem that is tough to handle, we resort to the greedy algorithms with low computational complexity. We propose a QoS constrained (QC) pilot allocation scheme, which sequentially allocates the pilot sequence having large interference power to the UE having small signal power so that the number of UEs satisfying QoS can be maximized and then the SE can also be maximized.

The notations are defined as follows. Symbols for matrices are denoted in boldface and upper case, while symbols for vectors are denoted in boldface and lower case. The symbols x, $\boldsymbol{x}$, $\boldsymbol{X}$ and $\mathcal{X}$ denote a scalar, a vector, a matrix and a set, respectively. The symbols $(\cdot)^T$, $(\cdot)^H$, $|\cdot|$, $\mathbb{E}[\cdot]$, $\mathbb{C}$, $\varnothing$ and $\boldsymbol{I}_K$ denote the transpose, the conjugate transpose (Hermitian), the absolute value, the expectation, the set of complex number, the empty set and the identity matrix with dimension of K, respectively. $K! \triangleq 1 \times 2 \times \cdots (K-1) \times K$ denote the factorial of K according to the convention. $\mathcal{CN}(m, \boldsymbol{R})$ denotes a complex Gaussian distribution with the mean and covariance matrix being m and $\boldsymbol{R}$, respectively.

II. System Model

We consider a multi-cell massive MIMO system with L cells, where each cell consists of an M-antenna BS and K single-antenna UEs ($M \geq K$).[1] We use the channel model given in [9] and the channel vector $\boldsymbol{h}_{ljk} \in \mathbb{C}^{M\times 1}$ from the kth UE in the jth cell to the BS in the lth cell for $l = 1, 2, \ldots, L,\ j = 1, 2, \ldots, L,\ k = 1, 2, \ldots, K$, is written as

$$\boldsymbol{h}_{ljk} = \sqrt{\beta_{ljk}}\boldsymbol{g}_{ljk}, \tag{1}$$

[1]If the numbers of UEs are different for different cells, we may assume that there are some virtual UEs whose large-scale coefficients are zero, so that all cells have the same number of UEs.

Manuscript received January 3, 2020; revised February 24, 2020; accepted March 9, 2020. Date of publication March 12, 2020; date of current version May 14, 2020. This work was supported in part by the National Natural Science Foundation of China under Grant 61871119, in part by the Natural Science Foundation of Jiangsu Province under Grant BK20161428, and in part by the Fundamental Research Funds for the Central Universities. The review of this article was coordinated by Prof. G. Gui. *(Corresponding author: Chenhao Qi.)*

Chenhao Qi and Xuyao Sun are with the School of Information Science and Engineering, Southeast University, Nanjing 210096, China (e-mail: qch@seu.edu.cn; sunxuyao@seu.edu.cn).

Yansha Deng is with the Department of Informatics, Kings College London, WC2R 2LS London, U.K. (e-mail: yansha.deng@kcl.ac.uk).

Arumugam Nallanathan is with the School of Electronic Engineering and Computer Science, Queen Mary University of London, E1 4NS London, U.K. (e-mail: anathan@qmul.ac.uk a.nall).

Digital Object Identifier 10.1109/TVT.2020.2980082

where β_{ljk} denoting the large-scale fading coefficient can be represented as

$$\beta_{ljk} = \frac{s_{ljk}}{(r_{ljk})^{\alpha}}. \tag{2}$$

s_{ljk} is the shadow fading coefficient following the logarithmic normal distribution with zero mean and variance being σ_{s}^2, i.e., $10\log_{10}(s_{ljk}) \sim \mathcal{CN}(0, \sigma_{\mathrm{s}}^2)$. r_{ljk} is the distance between the BS of the lth cell and the kth UE of the jth cell. α is the path loss factor. $\boldsymbol{g}_{ljk} \sim \mathcal{CN}(\boldsymbol{0}, \boldsymbol{I}_M)$ denotes the small-scale fading vector. Define $\boldsymbol{D}_{lj} \triangleq \mathrm{diag}\{\beta_{lj1}, \beta_{lj2}, \ldots, \beta_{ljK}\} \in \mathbb{C}^{K\times K}$ and $\boldsymbol{G}_{lj} \triangleq [\boldsymbol{g}_{lj1}, \boldsymbol{g}_{lj2}, \ldots, \boldsymbol{g}_{ljK}] \in \mathbb{C}^{M\times K}$. Then the channel matrix from all K UEs in the jth cell to the BS in the lth cell can be expressed as

$$\boldsymbol{H}_{lj} = \boldsymbol{G}_{lj}\boldsymbol{D}_{lj}^{1/2} \in \mathbb{C}^{M\times K}. \tag{3}$$

The widely used block fading channel model is employed in this work, where the channel matrix $\boldsymbol{H}_{lj}$ keeps constant within the channel coherence time.

During the uplink channel training, all UEs transmit pilot sequences to the BSs. Then the BSs estimate the corresponding channel matrices. Since the coherence time limits the number of available orthogonal pilot sequences, the pilot sequences used in the same cell are mutually orthogonal while all cells reuse the same group of orthogonal pilot sequences. We define the orthogonal pilot sequences used in each cell as $\boldsymbol{\Psi} \triangleq [\boldsymbol{\psi}_1^T, \boldsymbol{\psi}_2^T, \ldots, \boldsymbol{\psi}_K^T]^T \in \mathbb{C}^{K\times\tau}$, where

$$\boldsymbol{\Psi}\boldsymbol{\Psi}^H = \boldsymbol{I}_K \tag{4}$$

and $\boldsymbol{\psi}_k \in \mathbb{C}^{1\times\tau}$ denotes the kth pilot sequence with the length of τ. According to the existing pilot allocation scheme [15], the pilot sequence $\boldsymbol{\psi}_k$ is allocated to the kth UE in each cell regardless of different channel qualities of different UEs.

The received pilot signal $\boldsymbol{Y}_l^u \in \mathbb{C}^{M\times\tau}$ at the BS in the lth cell is expressed as [9]

$$\boldsymbol{Y}_l^u = \sqrt{\rho_p}\sum_{j=1}^{L}\boldsymbol{H}_{lj}\boldsymbol{\Psi} + \boldsymbol{N}_l, \tag{5}$$

where ρ_p denotes the average uplink pilot transmission power, $\boldsymbol{N}_l \sim \mathcal{CN}(\boldsymbol{0}, \sigma_n^2\boldsymbol{I}_M)$ is a Gaussian noise matrix. Then the BS in the lth cell uses matched filtering to estimate the channel matrix between the BS and all K UEs in the lth cell as

$$\widehat{\boldsymbol{H}}_{ll} = \frac{\boldsymbol{Y}_l^u\boldsymbol{\Psi}^H}{\sqrt{\rho_p}} = \sum_{j=1}^{L}\boldsymbol{H}_{lj} + \boldsymbol{Z}_l, \tag{6}$$

where $\boldsymbol{Z}_l \triangleq \boldsymbol{N}_l\boldsymbol{\Psi}^H/\sqrt{\rho_p}$ is the noise term. The second equality of (6) holds because of the orthogonality of the pilot sequences.

During the uplink data transmission, all UEs transmit data to their served BSs. Then the BSs detect the received data symbols with the estimated channel matrix. The received data symbol at the BS in the lth cell is expressed as

$$\boldsymbol{x}_l = \sqrt{\rho_u}\sum_{j=1}^{L}\boldsymbol{H}_{lj}\boldsymbol{s}_j + \boldsymbol{w}_l, \tag{7}$$

where ρ_u denotes the average uplink data transmission power, $\boldsymbol{s}_j \triangleq [s_{j1}, s_{j2}, \ldots, s_{jK}]^T \sim \mathcal{CN}(\boldsymbol{0}, \boldsymbol{I}_K)$ represents the symbol vector from K UEs in the jth cell, and $\boldsymbol{w}_l \sim \mathcal{CN}(\boldsymbol{0}, \sigma_n^2\boldsymbol{I}_M)$ denotes the additive white Gaussian noise (AWGN) vector.

By adopting the maximum ratio combining (MRC), the detected data symbol vector from K UEs in the lth cell can be written as

$$\boldsymbol{y}_l = \left(\sum_{j_1=1}^{L}\boldsymbol{H}_{lj_1} + \boldsymbol{Z}_l\right)^H\left(\sqrt{\rho_u}\sum_{j_2=1}^{L}\boldsymbol{H}_{lj_2}\boldsymbol{s}_{j_2} + \boldsymbol{w}_l\right). \tag{8}$$

Then the detected data symbol from the kth UE in the lth cell is given by

$$y_{lk} = \sqrt{\rho_u}\boldsymbol{h}_{llk}^H\boldsymbol{h}_{llk}s_{lk} + \mathrm{IRI}_k^u + \mathrm{IAI}_k^u + \varepsilon_k^u, \tag{9}$$

where the inter-cell multiuser interference is denoted as

$$\mathrm{IRI}_k^u \triangleq \sqrt{\rho_u}\sum_{\substack{j_1=1,j_2=1\\ \text{except } j_1=j_2=l}}^{L}\boldsymbol{h}_{lj_1\,k}^H\boldsymbol{H}_{lj_2}\boldsymbol{s}_{j_2}. \tag{10}$$

The noise term is denoted as

$$\varepsilon_k^u \triangleq \sum_{j_1=1}^{L}\boldsymbol{h}_{lj_1\,k}^H\boldsymbol{w}_l + \sqrt{\rho_u}\sum_{j_2=1}^{L}\boldsymbol{Z}_{lk}^H\boldsymbol{H}_{lj_2}\boldsymbol{s}_{j_2} + \boldsymbol{Z}_{lk}^H\boldsymbol{w}_l. \tag{11}$$

The intra-cell multiuser interference is denoted as

$$\mathrm{IAI}_k^u \triangleq \sqrt{\rho_u}\boldsymbol{h}_{llk}^H\sum_{t=1,t\neq k}^{K}\boldsymbol{h}_{llt}s_{lt}. \tag{12}$$

The average uplink SINR of the kth UE in the lth cell can be expressed as

$$\mathrm{SINR}_{lk}^u = \frac{\mathbb{E}\left\{\left|\sqrt{\rho_u}\boldsymbol{h}_{llk}^H\boldsymbol{h}_{llk}\right|^2\right\}}{\mathbb{E}\left\{\left|\mathrm{IAI}_k^u\right|^2\right\} + \mathbb{E}\left\{\left|\mathrm{IRI}_k^u\right|^2\right\} + \mathbb{E}\left\{\left|\varepsilon_k^u\right|^2\right\}}. \tag{13}$$

When M tends to infinity, we have

$$\mathbb{E}\left\{\left|\varepsilon_k^u\right|^2\right\} \xrightarrow{M\to\infty} 0, \tag{14}$$

$$\mathbb{E}\left\{\left|\sqrt{\rho_u}\boldsymbol{h}_{llk}^H\boldsymbol{h}_{llk}\right|^2\right\} \xrightarrow{M\to\infty} \rho_u M^2\beta_{llk}^2, \tag{15}$$

$$\mathbb{E}\left\{\left|\mathrm{IRI}_k^u\right|^2\right\} \xrightarrow{M\to\infty} \rho_u M^2\sum_{j=1,j\neq l}^{L}\beta_{ljk}^2, \tag{16}$$

$$\mathbb{E}\left\{\left|\mathrm{IAI}_k^u\right|^2\right\} \xrightarrow{M\to\infty} 0. \tag{17}$$

By substituting (14), (15), (16) and (17) into (13), we have

$$\lim_{M\to\infty}\mathrm{SINR}_{lk}^u = \frac{\beta_{llk}^2}{\sum_{j\neq l}\beta_{ljk}^2}. \tag{18}$$

Note that $\sum_{j\neq l}\beta_{ljk}^2$ represents the power of the inter-cell interference coming from the UEs using the kth pilot sequence in the other cells.

We define the asymptotic uplink SINR as

$$\mathrm{SINR}_{lk}^{u,\mathrm{asy}} \triangleq \frac{\beta_{llk}^2}{\sum_{j\neq l}\beta_{ljk}^2}. \tag{19}$$

Then the SE of the kth UE in the lth cell can be written as

$$R_{lk}^u = \log_2(1 + \mathrm{SINR}_{lk}^u) \tag{20}$$

and we have

$$\lim_{M\to\infty}R_{lk}^u = \log_2(1 + \mathrm{SINR}_{lk}^{u,\mathrm{asy}}) = \log_2\left(1 + \frac{\beta_{llk}^2}{\sum_{j\neq l}\beta_{ljk}^2}\right). \tag{21}$$

We define the asymptotic SE as

$$R_{lk}^{u,\mathrm{asy}} \triangleq \log_2\left(1+\frac{\beta_{llk}^2}{\sum_{j\neq l}\beta_{ljk}^2}\right). \tag{22}$$

It is seen that the pilot allocation will determine the asymptotic uplink SINR and further determine the asymptotic SE. Therefore, the SE depends on the large-scale fading coefficients as well as the pilot allocations when M grows to infinity.

III. Pilot Allocation Scheme

We consider the pilot allocation for the lth cell, which is regarded as the target cell. For the cells other than the target cell, the pilot allocation is individually performed by their corresponding BSs. Based on the data exchange among different cells, e.g., coordinated multiple points (CoMP), a specific BS can obtain the pilot allocation knowledge of other cells.

In multi-cell massive MIMO systems, we aim to maximize the SE of the uplink transmission for the target cell. To guarantee the requirement of the UEs, the QoS is an important metric. For example, if the UEs require video service, the QoS is high; if the UEs only require text service, the QoS is low. Therefore, we consider maximizing the number of UEs satisfying QoS in the target cell, based on which we further maximize the SE of the target cell. Then the bilevel optimization problem [16] to maximize the SE subject to the constraint that the number of users satisfying the QoS is maximized can be formulated as

$$\max_{\mathcal{F}_p\subseteq\mathcal{F}} \sum_{k=1}^{K} R_{lk}^{u}, \tag{23a}$$

$$\text{s.t. } \max_{\mathcal{F}_p\subseteq\mathcal{F}} \sum_{k=1}^{K} I(R_{lk}^{u}\geq\lambda_k) \tag{23b}$$

where $\mathcal{F}_p \triangleq [f_p^1, f_p^2, \ldots, f_p^K]$ denotes the pth kind of pilot allocation for $p=1,2,\ldots,K!$ and $\mathcal{F}$ denote all possible $K!$ kinds of pilot allocation. We define $I(x)$ to be a threshold function as

$$I(x)=\begin{cases}1, & x=1,\\ 0, & x=0.\end{cases} \tag{24}$$

It is seen that (23b) is the upper-level optimization problem which maximizes the number of QoS-satisfied UEs in the target cell. λ_k is the QoS threshold for the kth UE. (23a) is the lower-level optimization problem which maximizes the SE of the target cell.

It is difficult to solve such a bilevel optimization problem expressed in (23), since the computation of R_{lk}^{u} for each kind of pilot allocation consumes a large amount of computational resource. Fortunately, R_{lk}^{u} can be approximated by $R_{lk}^{u,\mathrm{asy}}$ as M goes to infinity, which means that $R_{lk}^{u}\approx R_{lk}^{u,\mathrm{asy}}$ holds in the massive MIMO setup with large M. Therefore R_{lk}^{u} can be represented by β_{ljk} and consequently can be fast computed. Note that β_{ljk} changes slowly and can be easily tracked by the BSs [17]. The BSs exchange the large-scale fading coefficients of the served UEs via limited BS cooperation, which is the same as that in [11]. After obtaining the large-scale fading coefficients of the UEs in the neighbouring cells, each BS independently performs the pilot allocation for the served UEs. Then (23) can be approximated by

$$\max_{\{\mathcal{F}_p\subseteq\mathcal{F}\}} \sum_{k=1}^{K} R_{lk}^{u,\mathrm{asy}}, \tag{25a}$$

$$\text{s.t. } \max_{\{\mathcal{F}_p\subseteq\mathcal{F}\}} \sum_{k=1}^{K} I(R_{lk}^{u,\mathrm{asy}}\geq\lambda_k). \tag{25b}$$

Algorithm 1: QC Pilot Allocation Algorithm.

1: **Input:** K, $\{\beta_{llk}^2\}_{k=1}^K$, $\{\sum_{j\neq l}\beta_{ljq}^2\}_{q=1}^K$.
2: Set $K'\leftarrow K$. $\mathcal{V}\leftarrow\varnothing$.
3: Set $\mathcal{K}\leftarrow\{1,2,\ldots,K\}$. $\mathcal{Q}\leftarrow\{1,2,\ldots,K\}$.
4: Obtain $\mathcal{S}\leftarrow\{\alpha_1,\alpha_2,\ldots,\alpha_K\}$. $\mathcal{I}\leftarrow\{\gamma_1,\gamma_2,\ldots,\gamma_K\}$.
5: **repeat**
6: **if** $\log_2(1+\alpha_1/\gamma_1)<\lambda$ **then**
7: $\mathcal{V}\leftarrow\{\mathcal{V},(\alpha_1,\gamma_{K'})\}$. $\mathcal{S}\leftarrow\mathcal{S}\backslash\{\alpha_1\}$. $\mathcal{I}\leftarrow\mathcal{I}\backslash\{\gamma_{K'}\}$.
8: **else if** $\log_2(1+\alpha_1/\gamma_1)\geq\lambda$ & $\log_2(1+\alpha_1/\gamma_{K'})<\lambda$ **then**
9: Obtain q^*.
10: $\mathcal{V}\leftarrow\{\mathcal{V},(\alpha_1,\gamma_{q^*})\}$. $\mathcal{S}\leftarrow\mathcal{S}\backslash\{\alpha_1\}$. $\mathcal{I}\leftarrow\mathcal{I}\backslash\{\gamma_{q^*}\}$.
11: **else**
12: $\mathcal{V}\leftarrow\{\mathcal{V},(\alpha_1,\gamma_{K'}),(\alpha_2,\gamma_{K'-1}),\ldots,(\alpha_{K'},\gamma_1)\}$.
13: Break.
14: **end if**
15: Update $K'\leftarrow K'-1$.
16: Update $\mathcal{K}\leftarrow\{1,2,\ldots,K'\}$. $\mathcal{Q}\leftarrow\{1,2,\ldots,K'\}$.
17: Update $\mathcal{S}$ and $\mathcal{I}$.
18: **until** $K'=0$
19: **Output:** $\mathcal{V}$.

The straightforward method to solve (25) is the exhaustive search, which tests all kinds of pilot allocation and selects the best one. Obviously, the exhaustive search results in unaffordable computational complexity. In this context, we resort to the greedy methods with much lower complexity. For simplicity, we assume $\lambda_1=\lambda_2=\cdots=\lambda_K=\lambda$ which means each UE has the same QoS threshold.

Here we propose a QoS constrained (QC) pilot allocation scheme. The detailed steps are summarized in Algorithm 1.

First we initialize the number of UEs to be allocated with pilots as $K'\leftarrow K$. We initialize the indices of UEs for pilot allocation to be $\mathcal{K}\leftarrow\{1,2,\ldots,K\}$. We initialize the indices of pilot sequences to be $\mathcal{Q}\leftarrow\{1,2,\ldots,K\}$. We rearrange $\beta_{llk}^2, k\in\mathcal{K}$, which indicates the signal power of $\mathrm{SINR}_{lk}^{u,\mathrm{asy}}$ for the kth UE in (19). Suppose the rearranged result is denoted as $\mathcal{S}\leftarrow\{\alpha_1,\alpha_2,\ldots,\alpha_K\}$, where $\alpha_1\leq\alpha_2\leq\cdots\leq\alpha_K$. Similarly, we rearrange $\sum_{j\neq l}\beta_{ljq}^2, q\in\mathcal{Q}$, which indicates the interference power of $\mathrm{SINR}_{lk}^{u,\mathrm{asy}}$ for the kth UE in (19). Suppose the rearranged result is denoted as $\mathcal{I}\leftarrow\{\gamma_1,\gamma_2,\ldots,\gamma_K\}$, where $\gamma_1\leq\gamma_2\leq\cdots\leq\gamma_K$. We use $\mathcal{V}$ to store the final result of the pilot allocation, where each entry of $\mathcal{V}$ denotes a combination of the signal power of the UE and the interference power of the corresponding allocated pilot. We initialize $\mathcal{V}$ to be an empty set, i.e., $\mathcal{V}\leftarrow\varnothing$.

Since the UE with smaller signal power has higher probability of violating QoS constraint, we give higher allocation priority to the UE with smaller signal power so that the number of UEs satisfying QoS can be maximized according to (25b). We start allocating pilot for the UE with the smallest signal power denoted as α_1.

If $\log_2(1+\alpha_1/\gamma_1)<\lambda$, no matter which pilot is allocated, the QoS of the corresponding UE cannot be satisfied. In this context, we allocate the pilot with the largest interference power $\gamma_{K'}$ to the UE with the smallest signal power α_1, giving the chances to the other UEs. As shown in step 5 of Algorithm 1, we add $(\alpha_1,\gamma_{K'})$ to $\mathcal{V}$, and then remove α_1 and $\gamma_{K'}$ from $\mathcal{S}$ and $\mathcal{I}$, respectively.

If $\log_2(1+\alpha_1/\gamma_1)\geq\lambda$ and $\log_2(1+\alpha_1/\gamma_{K'})<\lambda$, we use the bisection search method to find the pilot indexed as q^* which satisfies $\log_2(1+\alpha_1/\gamma_{q^*})\geq\lambda$ and $\log_2(1+\alpha_1/\gamma_{q^*+1})<\lambda$. Note that any pilot with interference power $\{\gamma_1,\gamma_2,\ldots,\gamma_{q^*}\}$ can be allocated to the UE with signal power α_1 to satisfy QoS constraint. In order to give more chances to the other UEs, we allocate the pilot with interference

TABLE I
SIMULATION PARAMETERS

Number of cells L	7
Number of BS antennas M	$100 \leq M \leq 1000$
Number of UEs in each cell K	8
Cell radius R	1000 m
Path loss exponent α	3
Log-normal shadowing fading σ_{s}	8 dB
Transmit power of pilots and data ρ_p, ρ_u	0 dBm
Uplink SNR	20 dB

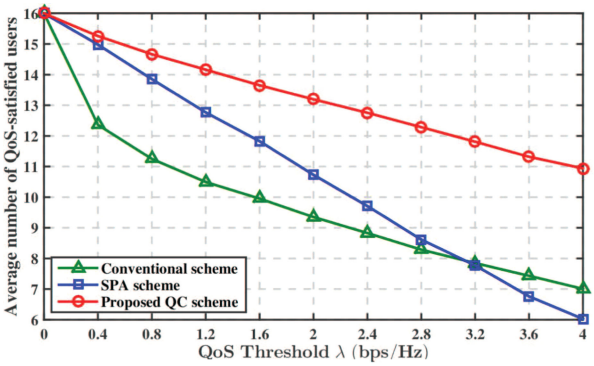

Fig. 1. Comparisons of average number of QoS-satisfied UEs for different pilot allocation schemes in terms of the QoS threshold λ.

power γ_{q^*} to the UE with signal power α_1. As shown in step 8, we add (α_1, γ_{q^*}) to $\mathcal{V}$, and then remove α_1 and γ_{q^*} from $\mathcal{S}$ and $\mathcal{I}$, respectively.

If $\log_2(1 + \alpha_1/\gamma_{K'}) \geq \lambda$, the QoS constraint of the remaining UEs can be satisfied no matter how the remaining pilots are allocated. According to (25a) which maximizes the SE, we form the combinations $(\alpha_1, \gamma_{K'})$, $(\alpha_2, \gamma_{K'-1})$, $\ldots$, $(\alpha_{K'}, \gamma_1)$ and add them to $\mathcal{V}$, as shown in step 10. After that, we break the iteration and output the result of the pilot allocation.

After completing the pilot allocation for the UE with signal power α_1, we update $K' \leftarrow K' - 1$ and correspondingly $\mathcal{K} \leftarrow \{1, 2, \ldots, K'\}$ and $\mathcal{Q} \leftarrow \{1, 2, \ldots, K'\}$, which indicates that the number of UEs to be allocated with pilots is decreased by one. In addition, we rearrange the remaining UE set and pilot set as $\mathcal{S} \leftarrow \{\alpha_1, \alpha_2, \ldots, \alpha_{K'}\}$ and $\mathcal{I} \leftarrow \{\gamma_1, \gamma_2, \ldots, \gamma_{K'}\}$, respectively. We repeat the above steps until the pilot allocation is finished for all the UEs, i.e., $K' = 0$. Finally, we output $\mathcal{V}$ as the result of the pilot allocation.

For the computational complexity, the proposed QC scheme is the same as SPA to be $\mathcal{O}(K^2)$, while it is $\mathcal{O}(K!)$ for the exhaustive search. Apparently, the exhaustive search has much higher computational complexity when $K \geq 5$.

IV. SIMULATION RESULTS

The considered multi-cell massive MIMO system includes L cells, where each cell has a BS with M antennas serving K single-antenna UEs. The center cell with six neighbouring cells is named as the target cell. The detailed parameters of the multi-cell massive MIMO system for the simulations are summarized in Table I. We run the Monte Carlo simulations with 5000 random channel implementations.

As shown in Fig. 1, we compare the average number of QoS-satisfied UEs in the target cell for different pilot allocation schemes in terms of different QoS threshold λ. We set the number of BS antennas as $M = 300$. The comparisons include the conventional scheme [15] which simply allocates the pilot sequence $\boldsymbol{\psi}_k$ to the kth UE, the SPA scheme [11] and the proposed QC scheme. It is seen that the proposed

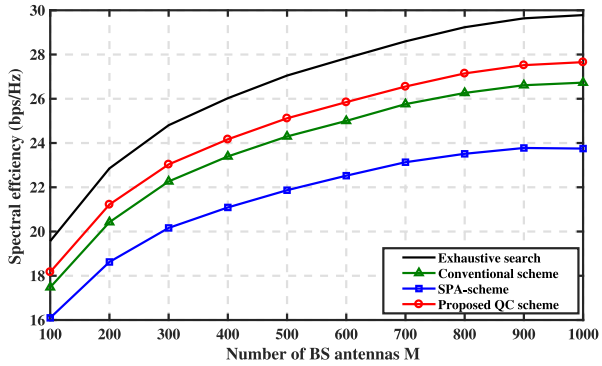

Fig. 2. Comparisons of SE for different pilot allocation schemes with different number of BS antennas M.

QC scheme outperforms the SPA scheme and the conventional scheme. In particular, at $\lambda = 2$ bps/Hz, the proposed QC scheme has 2.46 and 3.84 average number of QoS-satisfied UEs improvement over the SPA scheme and the conventional scheme, respectively.

As seen from Fig. 2, we compare the uplink SE in the target cell for different pilot allocation schemes in terms of different number of BS antennas M. To show the performance upper bound, we also provide the simulation results of exhaustive search. We set $\lambda = 2$ bps/Hz. As M gets larger, the SE of all schemes increases. We can observe that the QC scheme outperforms the SPA scheme and the conventional scheme, and only suffer small performance loss compared with the exhaustive search. In particular, at $M = 800$, the proposed QC scheme has 5.22% and 16.07% SE improvement over the conventional scheme and the SPA scheme respectively, and only 7.14% SE reduction compared with the exhaustive scheme. In terms of the computational complexity, our scheme is the same as SPA and is only 0.15% of the exhaustive search.

V. CONCLUSION

To make a short summary, we have investigated pilot allocation scheme aiming to maximize the SE subject to the constraint that the number of the UEs satisfying the QoS is maximized. For the considered bilevel optimization problem that is tough to handle, we have resorted to the greedy algorithms with low computational complexity. We have proposed the QC pilot allocation scheme, which sequentially allocates the pilot sequence having large interference power to the UE having small signal power so that the number of UEs satisfying QoS can be maximized and then the SE can also be maximized. Our future work will focus on the pilot allocation under other criterions such as user fairness.

REFERENCES

[1] Z. Wan, Z. Gao, B. Shim, K. Yang, G. Mao, and M. Alouini, "Compressive sensing based channel estimation for millimeter-wave full-dimensional MIMO with lens-array," *IEEE Trans. Veh. Technol.*, vol. 69, no. 2, pp. 2337–2342, Feb. 2020.

[2] K. Chen, C. Qi, and G. Y. Li, "Two-step codeword design for millimeter wave massive MIMO systems with quantized phase shifters," *IEEE Trans. Signal Process.*, vol. 68, no. 1, pp. 170–180, Jan. 2020.

[3] H. Huang, Y. Song, J. Yang, G. Gui, and F. Adachi, "Deep-learning-based millimeter-wave massive MIMO for hybrid precoding," *IEEE Trans. Veh. Technol.*, vol. 68, no. 3, pp. 3027–3032, Mar. 2019.

[4] W. Ma, C. Qi, Z. Zhang, and J. Cheng, "Sparse channel estimation and hybrid precoding using deep learning for millimeter wave massive MIMO," *IEEE Trans. Commun.*, to be published, doi: 10.1109/TCOMM.2020.2974457.

[5] M. Liu, T. Song, and G. Gui, "Deep cognitive perspective: Resource allocation for NOMA-based heterogeneous IoT with imperfect SIC," *IEEE Internet Things J.*, vol. 6, no. 2, pp. 2885–2894, Apr. 2019.
[6] S. Ma, Y. He, H. Li, S. Lu, F. Zhang, and S. Li, "Optimal power allocation for mobile users in non-orthogonal multiple access visible light communication networks," *IEEE Trans. Commun.*, vol. 67, no. 3, pp. 2233–2244, Mar. 2019.
[7] M. Ke, Z. Gao, Y. Wu, X. Gao, and R. Schober, "Compressive sensing-based adaptive active user detection and channel estimation: Massive access meets massive MIMO," *IEEE Trans. Signal Process.*, vol. 68, pp. 764–779, Jan. 2020, doi: 10.1109/TSP.2020.2967175.
[8] L. Lu, G. Y. Li, A. L. Swindlehurst, A. Ashikhmin, and R. Zhang, "An overview of massive MIMO: Benefits and challenges," *IEEE J. Sel. Topics Signal Process.*, vol. 8, no. 5, pp. 742–758, Oct. 2014.
[9] T. L. Marzetta, "Noncooperative cellular wireless with unlimited numbers of base station antennas," *IEEE Trans. Wireless Commun.*, vol. 9, no. 11, pp. 3590–3600, Nov. 2010.
[10] F. Rusek *et al.*, "Scaling up MIMO: Opportunities and challenges with very large arrays," *IEEE Signal Process. Mag.*, vol. 30, no. 1, pp. 40–60, Jan. 2013.
[11] X. Zhu, Z. Wang, L. Dai, and Q. Chen, "Smart pilot assignment for massive MIMO," *IEEE Commun. Lett.*, vol. 19, no. 9, pp. 1644–1647, Sep. 2015.
[12] S. Ma, E. L. Xu, A. Salimi, and S. Cui, "A novel pilot assignment scheme in massive MIMO networks," *IEEE Wireless Commun. Lett.*, vol. 7, no. 2, pp. 262–265, Apr. 2018.
[13] K. Kim, J. Lee, and J. Choi, "Deep learning based pilot allocation scheme (DL-PAS) for 5G massive MIMO system," *IEEE Commun. Lett.*, vol. 22, no. 4, pp. 828–831, Apr. 2018.
[14] X. Zhu, L. Dai, Z. Wang, and X. Wang, "Weighted-graph-coloring-based pilot decontamination for multicell massive MIMO systems," *IEEE Trans. Vech. Technol.*, vol. 66, no. 3, pp. 2829–2834, Mar. 2017.
[15] F. Fernandes, A. Ashikhmin, and T. L. Marzetta, "Inter-cell interference in noncooperative TDD large scale antenna systems," *IEEE J. Sel. Areas Commun.*, vol. 31, no. 2, pp. 192–201, Feb. 2013.
[16] A. Sinha, P. Malo, and K. Deb, "A review on bilevel optimization: From classical to evolutionary approaches and applications," *IEEE Trans. Evol. Comput.*, vol. 22, no. 2, pp. 276–295, Apr. 2018.
[17] R. R. Muller, L. Cottatellucci, and M. Vehkapera, "Blind pilot decontamination," *IEEE J. Sel. Topics Signal Process.*, vol. 8, no. 5, pp. 773–786, Oct. 2014.